Reviewed research article

A data set of gridded daily temperature in Iceland, 1949–2010

Philippe Crochet and Tómas Jóhannesson

Icelandic Meteorological Office, Bústaðavegur 9, IS-150 Reykjavík, Iceland

Corresponding author: philippe@vedur.is

Abstract — *A high spatial resolution data set of gridded daily surface air temperature in Iceland has been derived for the period 1949–2010. Between 60–80% of the daily estimates are within* $\pm 1\,^{\circ}\mathrm{C}$ *depending on the month of the year and between 90–95% are within* $\pm 2\,^{\circ}\mathrm{C}$ *of independent station measurements in 1995–2010. The data set is thus well suited for various hydrological, glaciological and climatological modelling studies. The quality of the gridded data set is found to be best near the coast because of the higher station density. Including data from automatic stations, the establishment of which started in the early 90's, was found to improve the data set. Derived 30-year mean monthly maps compare favourably with reference maps derived directly from monthly mean station temperatures with more sophisticated statistical techniques. An analysis of decadal temperature variations based on the data set shows that the decade 2001–2010 was the warmest of the last 60 years and makes it possible to identify spatial patterns in the decadal variations. As an example, the spatial distribution of the warming of recent decades shows that it is more pronounced in the inland compared with coastal areas.*

INTRODUCTION

Knowledge of the spatio-temporal distribution of surface air temperature and precipitation in the complex terrain of Iceland is important for various applications ranging from local and regional climate monitoring to hydrological and glaciological modelling studies at the catchment scale. Gridded data sets with a high temporal resolution and a good spatial coverage are particularly suitable for modelling because they bridge gaps in the station network and do not depend directly on the operation of observing stations at various locations.

Glacier mass balance studies in Iceland are often carried out with simple temperature-index melt models using extrapolated temperature and precipitation from single station measurements employing fixed horizontal and vertical temperature and precipitation gradients (Jóhannesson *et al.*, 1995; Jóhannesson, 1997; Aðalgeirsdóttir *et al.*, 2006). The accuracy of this type of modelling could be improved with accurate gridded temperature and precipitation estimates, in particular for mass balance modelling of the 8100 km^2 Vatnajökull ice cap where the single station approach is clearly inadequate. Gridded data sets are also useful for mass balance modelling of glaciers that are far away from meteorological stations and where station measurements are missing for single days or longer periods due to instrument failures or other reasons.

Hydro-glaciological models that simulate the response of small to medium-sized river catchments in complex terrain often need to operate at high spatio-temporal resolutions, typically 1 km and 1 day, because the variability of precipitation and temperature is large and response times are short. Snow and glaciers in particular play an important role in the flow regime characteristics of many Icelandic rivers and runoff generation depends to a great extent on the interplay of rain and the melting of snow and ice (Jónsdóttir *et al.*, 2008). Under these conditions, it is important to estimate the spatial distribution of precipitation and temperature accurately in order to properly distinguish between rainfall and snowfall and adequately estimate the snowpack evolution and the timing and magnitude of snow and glacier melt.

Accurate estimates of meteorological input information is crucial for robust calibration of hydro-glaciological models and to avoid the introduction of noise and bias related to this input information. This is especially important in the context of climate change impact studies where models calibrated for the present climate are used to simulate future water resources (Bergström *et al.*, 2007; Jóhannesson *et al.*, 2007; Jónsdóttir, 2008; Einarsson and Jónsson, 2010).

While gridded precipitation fields with high spatio-temporal resolution have recently been constructed for Iceland (Crochet *et al.*, 2007; Jóhannesson *et al.*, 2007), similar temperature data sets have not been available.

A large number of methods of different complexity have been proposed to interpolate climate data and in particular temperature from sparse observations (see for instance Bolstad *et al.*, 1998; Gozzini *et al.*, 2000; Price *et al.*, 2000; Hasenauer *et al.*, 2003; Apaydin *et al.*, 2004; Chuanyan *et al.*, 2005; Daly, 2006; Björnsson *et al.*, 2007). Several of these are based on simple interpolation methods such as inverse-distance weighting or truncated Gaussian weighting filters. Others are based on more advanced methods such as spline-surface fitting and various forms of kriging. One of the advantages of kriging is the use of a spatial covariance function or semi-variogram that describes the spatial variability of the data, but in the context of daily temperature mapping over several decades, estimating such a function for each day is non-trivial although automatic structural identification can be used. Methods exist though to minimize the needed computational effort, based on the calculation of a so-called climatological semi-variogram (Creutin and Obled, 1982; Lebel *et al.*, 1987). As terrain features are known to strongly influence temperature variations (Daly, 2006), direct spatial interpolation in mountainous terrain is problematic except for very high station densities. Both kriging and spline-based methods can take other explanatory variables such as elevation into account. Examples are co-kriging (Phillips *et al.*, 1992; Pardo-Iguzquiza, 1998), kriging with an external drift (Hudson and Wackernagel, 1994; Pardo-Iguzquiza, 1998) and trivariate thin-plate smoothing splines (Sharples *et al.*, 2005).

Another way to take the effect of elevation on temperature into account is to use the so-called lapse-rate method. The temperature at a given location is estimated by adjusting measured temperature at a nearby station given their respective elevation difference and an appropriate temperature gradient (see for instance Bolstad *et al.*, 1998). However, factors other than elevation can influence spatial temperature variations, especially in complex terrain. These spatial variations may be due to orographic effects such as temperature inversions resulting from cool air drained and trapped into valley depressions, sharp temperature gradients between air masses separated by topographic barriers, local orographic effects such as different slope aspects leading to a different amounts of incoming solar radiation, coastal effects leading to temperature contrasts between ocean and adjacent land masses, and land use/landcover variations (Bolstad *et al.*, 1998; Chuanyan *et al.*, 2005; Daly, 2006). For this reason, multiple linear regression models that formulate statistical relationships between temperature and local or regional orographic, geographic and landscape factors have been proposed and often used for estimating long-term averaged temperature in combination with residual interpolation such as detrended kriging, to account for spatial variations not described by the regression analysis. Such a method was used by Tveito *et al.* (2000) and by Björnsson *et al.* (2007) to estimate the 1961–1990 mean monthly seasonal and annual temperature in Iceland. However, these relationships may be cumbersome to derive for each day and not necessarily valid or as accurate as for long-term means. One possible solution for obtaining daily temperature fields in complex terrain is to combine the use of such method applied on long-term averages and anomaly interpolation (see for instance the use of the Aurelhy method in Gozzini *et al.*, 2000).

This paper presents a gridded daily temperature data set for Iceland with a 1 km resolution and evaluates its quality. The study is organized as follows.

First, the data and methods are presented, then a validation is performed by comparing the interpolated fields with independent station observations and a reference climatology, followed by a section presenting decadal anomaly maps over the past 60 years.

DATA AND METHODS

Data

The present analysis relies on several data sources: i) the station network operated by the Icelandic Meteorological Office (IMO) which consists of manned and automatic stations, a network of automatic stations operated by ii) the Icelandic Road Administration (ICERA), iii) Landsvirkjun (The National Power Company), iv) The National Energy Authority (NEA), v) the Icelandic Maritime Administration (IMA), and vi) local harbors. Daily temperature is calculated from 00UTC to 00UTC each day. For the automatic stations, it is a simple average of all measurements made during this 24-h period. For the manned stations, the measurements are performed at a 3-hourly interval but depending on the station not all the 3-hourly measurements are made so that the daily temperature is calculated by a weighted sum in order to take into account the daily temperature cycle (see Appendix 1 in Hovmöller, 1960). The stations have been split into three groups: group-1 includes all manned stations, group-2 includes automatic stations from IMO, Landsvirkjun, NEA, IMA and harbors, and group-3 includes automatic stations from ICERA. Automatic weather stations operated on the ice caps of Iceland by the Earth Science Institute of the University of Iceland in recent years are not used in this analysis because of the different characteristics of 2 m temperature measurements over glaciers compared with measurements on ice-free land (see below).

The number of stations in operation has varied considerably during the period under study, 1949–2010 (Figure 1). The number of manned stations reached a maximum near the end of the 1980s, followed by a gradual decline, compensated by the growing installation of automatic stations after the mid-90s (Figure 1a). Until the 1960s, the network was mainly located along the coastline (Figure 1b), in the 1980s it expanded into the SW and NE highlands (Figure 1c), and after 2000, the spatial coverage has improved further, especially in the highlands, around the glaciers and in the mountains near the coast in SW-, NW-, N- and SE-Iceland (Figure 1d). Note, however, that as group-3 stations are mainly located along roads, they are rather few in the central highlands.

The station density, estimated as the average number of neighbouring stations within 50 and 100 km of each station is summarized in Table 1. The calculation is done for each station individually and each day before the statistics are averaged over all stations. Table 2 gives information about the network elevation estimated on the 15$^{\text{th}}$ of June for years 1950, 1960, 1970, 1980, 1990, 2000, and 2010 respectively. For the manned stations, the distribution is quite asymmetrical, with 50% of stations located below 25 m a.s.l. and a mean elevation around 65 m a.s.l, in average. There is a drop in the maximum elevation in 2010 after manned observations at Hveravellir in central Iceland were terminated. The automatic stations of group-2 have a median elevation of 50 m a.s.l. and a mean elevation of 224 m a.s.l., in average, while group-3 stations have a more symmetrical distribution with a median and mean elevations around 240 m a.s.l. To summarize, the table indicates that weather stations are mainly located at comparatively low elevations, especially the manned stations, but automatic stations have been deployed at progressively higher elevations in the highlands in recent years. For comparison, a 1-km digital elevation model (DEM) indicates that the mean elevation of Iceland is 503 m a.s.l. and the median 472 m a.s.l. 10% of land grid points are below 45 m a.s.l. and 10% above 992 m a.s.l.

Estimates of 2-m temperature over glaciers are associated with special methodological problems. A melting snow or ice surface will maintain a maximum skin or 0-m temperature of 0°C irrespective of the temperature of the surrounding air mass. This leads to steep vertical temperature gradients through the boundary layer near the glacier surface on warm summer days and the 2-m temperature will be very dependent on wind conditions and vertical mixing in the boundary layer. In fact, large variations in measured 2-m temperature over an ablating glacier surface may

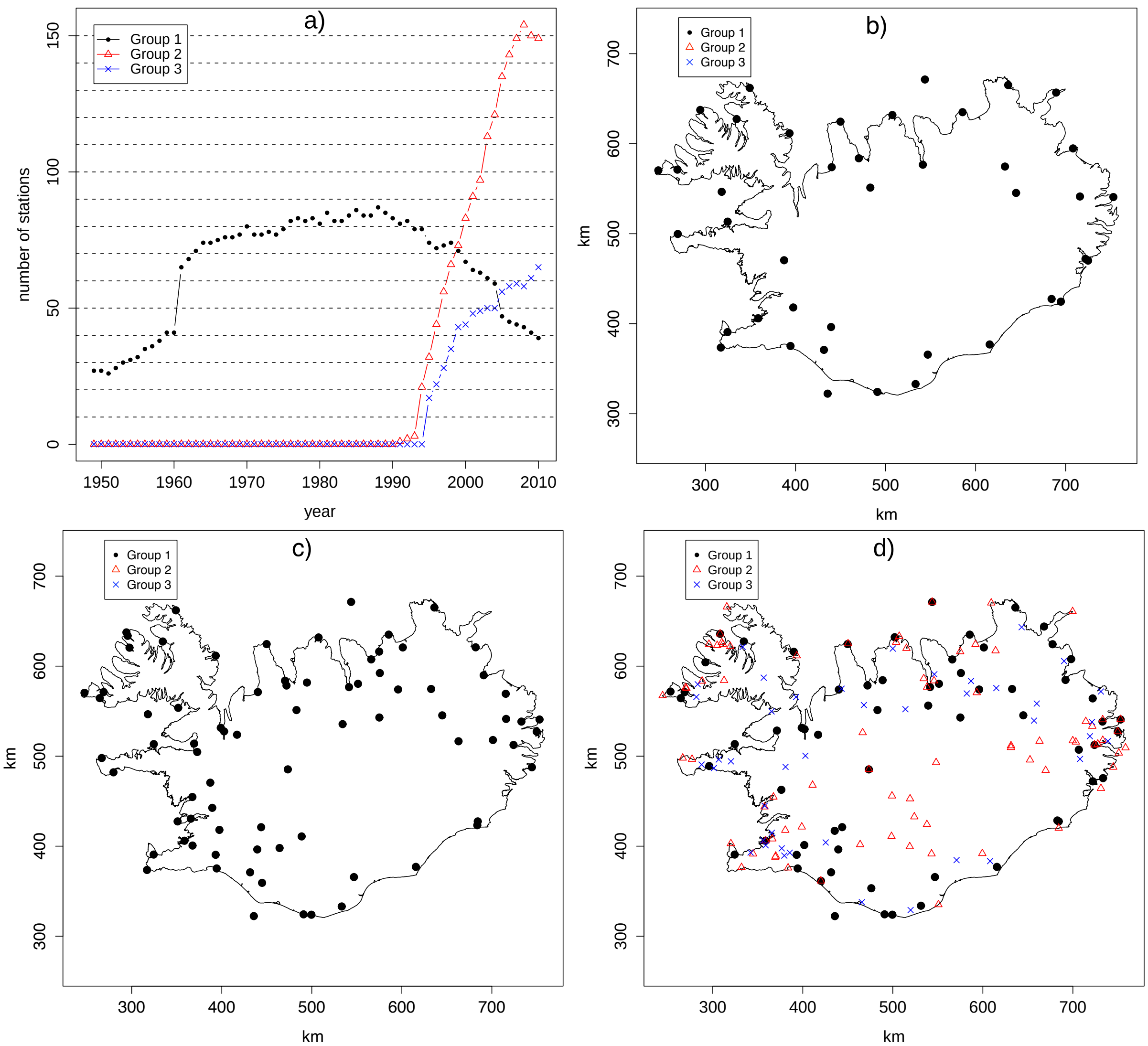

Figure 1. Network development for group-1 stations (circles), group-2 stations (triangles), and group-3 stations (crosses) (a). Network in 1960 (b), 1980 (c) and 2000 (d). – *Þróun veðurstöðvamælinetsins fyrir stöðvar í flokki 1 (hringir), flokki 2 (þríhyrningar), og flokki 3 (krossar) (a). Staðsetning veðurstöðva árið 1960 (b), 1980 (c) and 2000 (d).*

be caused by changes in wind speed, such as when Foehn winds induce break-up of the near-surface inversion (Obleitner, 2000). The 2-m temperature will under such conditions be rather problematic as a prognostic variable in simple melt models such as degree–day models because it does not represent or reflect the temperature of the surrounding air mass (Guðmundsson *et al.*, 2009). The station temperatures used to estimate the gridded temperature fields derived in this paper are all from outside the glaciers and do therefore not reflect conditions related to the near-surface boundary layer on the glaciers. This implies that the

Table 1. Average number of stations within 50 (100) km of group-2 and group-3 stations. – *Fjöldi veðurstöðva innan 50 (100) km frá stöðvum í flokki 2 og flokki 3.*

Statistics	Min	25%	Median	Mean	75%	Max
Nb. of G-1 st. near G-2 st.	0 (1)	1.4 (3.9)	2.6 (5.4)	2.6 (5.8)	3.5 (7.2)	6.4 (11.4)
Nb. of G-1 st. near G-3 st.	0.7 (0.8)	2.5 (4.5)	3.2 (6.1)	3.4 (6.2)	4.0 (7.6)	6.8 (15.5)
Nb. of G-1 and G-2 st. near G-3 st.	2.9 (7.9)	5.8 (14.0)	7.5 (17.7)	10.4 (18.5)	15.2 (22.0)	27.2 (38.2)

Table 2. Station elevation statistics (in m a.s.l.). – *Hæð veðurstöðva (í m y.s.).*

Statistics/Period	1950	1960	1970	1980	1990	2000	2010
25% (Group-1)	14	12	13	14	15	16	14
Median (Group-1)	23	20	27	27	25	25	25
Mean (Group-1)	48	50	75	76	73	71	60
75% (Group-1)	44	39	80	79	83	52	50
Max (Group-1)	384	450	672	641	641	641	384
25% (Group-2)	NA	NA	NA	NA	NA	10	16
Median (Group-2)	NA	NA	NA	NA	NA	48	52
Mean (Group-2)	NA	NA	NA	NA	NA	230	219
75% (Group-2)	NA	NA	NA	NA	NA	550	450
Max (Group-2)	NA	NA	NA	NA	NA	949	949
25% (Group-3)	NA	NA	NA	NA	NA	40	44
Median (Group-3)	NA	NA	NA	NA	NA	267	226
Mean (Group-3)	NA	NA	NA	NA	NA	252	231
75% (Group-3)	NA	NA	NA	NA	NA	397	370
Max (Group-3)	NA	NA	NA	NA	NA	600	600

temperature fields should not be interpreted as representing the actual 2-m temperature over glaciers on warm days when melting of snow or ice takes place. Rather, the gridded temperatures may be interpreted as an estimate of the 2-m air temperature over a hypothetical ice-free surface at the location and altitude in question. It could be argued that the temperature estimates obtained here for the glaciers should be masked out from the gridded temperature fields because they do not represent an unbiased estimate of the in-situ 2-m temperature that would be measured by a weather station located on the glacier surface as explained above. Rather than doing this, we provide a mask on the same grid identifying the glacier-covered areas of Iceland so that the users can mask out temperatures over glaciers if they so choose. The temperature estimated here for the glaciers based only on measurements outside the glaciers are as mentioned above useful for various modelling purposes and are therefore a valuable part of the data set. We also note that other gridded temperature data sets for Iceland (e.g. the data set of Björnsson *et al.*, 2007) are also based on measurements from outside the glaciers and will therefore be similar to our data set in this regard.

Gridding method

The method used to construct the gridded temperature fields is similar to the one used by Dodson and Marks (1997), the so-called linear lapse rate adjustment. It combines a spatial interpolation technique with an elevation correction based on a spatially constant lapse-rate. This method has been used at IMO over the past 10 years to produce 3-hourly temperature maps in near real time for the purpose of weather monitoring (unpublished work). First, as temperature is known to be influenced by elevation (Daly, 2006), elevation differences between stations are corrected by estimating sea-level temperature at the location of each station with a vertical lapse rate dT/dz. The estimated sea-level temperature is then gridded onto a 1-km mesh using a tension-spline interpolation which is a generalization of the minimum-curvature method in which large oscillations and extraneous inflection points are eliminated by adding tension to the elastic-plate flexure equation (Smith and Wessel, 1990). This method offers a relatively high level of sophistication without requiring the selection and estimation of a covariance function or semi-variogram for each day which would have required much more computational effort without necessarily obtaining substantially better results, especially for periods when the network density is sparse. Finally, the gridded sea-level temperature is adjusted to the terrain elevation with the same vertical lapse rate using a DEM with the same 1-km grid mesh. No attempt was made here to capture other types of spatial variations, for example related to distance to the coast or surface characteristics other than elevation.

Four different sets of gridded temperature fields were constructed. Two sets were made using manned stations (group-1) only by applying i) a spatially and temporally constant vertical lapse rate and ii) a spatially constant but temporally variable lapse rate. Two additional sets were calculated by adding the data from the group-2 automatic stations installed after 1995 using the same two sets of lapse rates, respectively.

The temporally constant lapse rate was somewhat arbitrarily chosen as $6.5\,^{\circ}$C/km. This lapse rate is often considered to represent the average vertical temperature gradient in the troposphere (Stone and Carlson, 1979; Engen-Skaugen, 2007; Li and Williams, 2008) and it has often been used in glaciological and hydrological studies to adjust temperature measurements over catchment areas (see for instance Michlmayr *et al.*, 2008; Hebeler and Purves, 2008). The monthly variable lapse rate (Table 3) was taken from Tveito *et al.* (2000), where this lapse rate was calculated as one of the components of a multiple linear regression (MLR) analysis between temperature and various topographic and geographic factors. This lapse rate estimate could, however, be influenced by the presence of other variables in the MLR relationship. The lapse rate of Tveito *et al.* (2000) displays a seasonal pattern. It is close to dry-adiabatic in the winter and spring seasons and close to the standard value adopted in this study, in summer.

The gridded temperature fields obtained as described above are based on a regular 1x1 km grid of the topography of Iceland. This is a rather high spatial resolution for many applications but errors due to errors in the assumed topography may arise in some applications if temperatures for a particular point location are interpolated directly from the gridded temperatures. In general, it is recommended that temperature estimates for point locations with a known altitude are corrected for the difference between the known altitude of the point in question and the interpolated altitude from the 1x1 km grid of Iceland, which for this reason is included as an integral part of the data set (using a lapse rate of $6.5\,^{\circ}$C/km). Estimated station temperatures used in the validation described below are calculated in this manner.

VALIDATION

The gridded temperature fields were evaluated over the period 1995–2010 against independent stations whose measurements were not used in the spatial interpolation. The first two data sets made with the manned network only (group-1) were verified against group-2 stations and group-3 stations. The other two

Table 3. Variable lapse rates in °C/km derived from Tveito *et al.* (2000). – *Breytilegt hitafall með hæð í °C/km skv. Tveito o.fl. (2000).*

Period	Jan	Feb	Mar	Apr	May	Jun	Jul	Aug	Sep	Oct	Nov	Dec
lapse rate	9.7	9.6	8.9	9.7	9.3	7.9	7.1	7.0	7.5	8.0	9.4	9.4

data sets made by combining group-1 and group-2 stations were verified against group-3 stations. The evaluation was made for each month separately, considering first all stations together and then two altitude ranges separately, below and above 300 m a.s.l. The basic statistical criteria used were the Mean Error (ME), Mean Absolute Error (MAE), Root-Mean Square Error (RMSE) and the error frequency distribution. The error is taken as observed minus predicted temperature. Finally, 1961–1990 mean monthly and annual temperature fields were computed from the daily fields using manned stations only and compared with 1961–1990 mean monthly and annual temperature fields calculated by Björnsson *et al.* (2007) with residual kriging. Björnsson's *et al.* temperature maps, originally constructed on a regular lat–lon grid with half a minute resolution have been re-interpolated on the 1-km grid applied here using tension splines.

Verification against independent stations using a constant lapse rate

Figure 2 presents ME, MAE and RMSE for each month. The largest ME is observed from March to June and is always negative, meaning that the estimated temperature is warmer than the observed one. For the other months, ME is within $\pm 0.1\,^{\circ}$C, but mainly positive. A t-test (not shown) confirmed that the ME was significantly different from $0\,^{\circ}$C at a 5% significance level, except in January, July, September, October and November for estimates made at group-2 stations with group-1 stations, in February for estimates made at group-3 stations with group-1 stations and in October for estimates made at group-3 stations with group-1 and group-2 stations.

Both MAE and RMSE describe the same seasonality with larger values in winter than in summer. This seasonality could be related to a lapse rate seasonality, indicating that a constant standard lapse rate

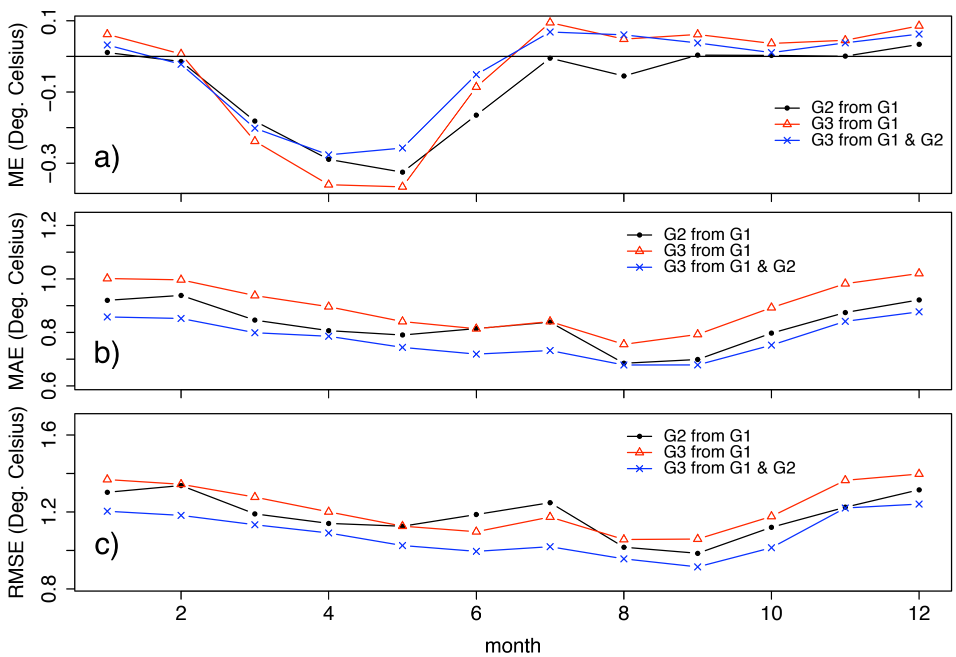

Figure 2. Error statistics using a constant lapse rate: ME (a), MAE (b) and RMSE (c). Error statistics at group-2 stations using group-1 stations (circles), group-3 stations using group-1 stations (triangles), group-3 stations using group-1 and group-2 stations (crosses). – *Tölfræðileg dreifing skekkju í reiknuðum hita fyrir fast hitafall með hæð.*

of 6.5 °C/km is closer to the actual average monthly lapse rate in summer than in winter. These results could also indicate that variations in the lapse rate in space and time are larger in winter than in summer. The MAE ranges between 0.7 °C and 1 °C, and the RMSE ranges between 0.9 °C and 1.4 °C.

When errors are estimated using fields derived from group-1 stations, MAE and RMSE are usually slightly larger at group-3 stations than at group-2 stations. According to Table 1, the station density of group-1 stations within 50 km of group-2 stations is slightly lower, in average, than around group-3 stations and also within a radius of 100 km. However, the elevation of group-3 stations, is higher in average than group-1 and group-2 stations (Table 2), and vertical adjustment errors could also account for these results. The benefit of the increased station density after 1995 by combining the manual and automatic stations is evident and one can see that MAE and RMSE are reduced by about 0.1 °C in average for all months and ME is reduced for all months except in February and August.

The proportion of error within several temperature ranges is presented in Figure 3. The best scores are obtained in summer and the worst in winter, in line with MAE and RMSE. Between 34–52% of the daily estimates are within ±0.5 °C, between 60–78% are within ±1 °C and between 88–96% are within ±2 °C depending on the month of the year.

Figures 4 and 5 present ME and MAE for stations below and above 300 m a.s.l., respectively. Below 300 m a.s.l., ME is negative from April to August at group-2 stations and positive the rest of the time, while at group-3 stations, ME is negative from April to July and positive the rest of the time for fields based on group-1 stations and mostly positive for fields based on group-1 and group-2 stations except in April and May. The average error ranges

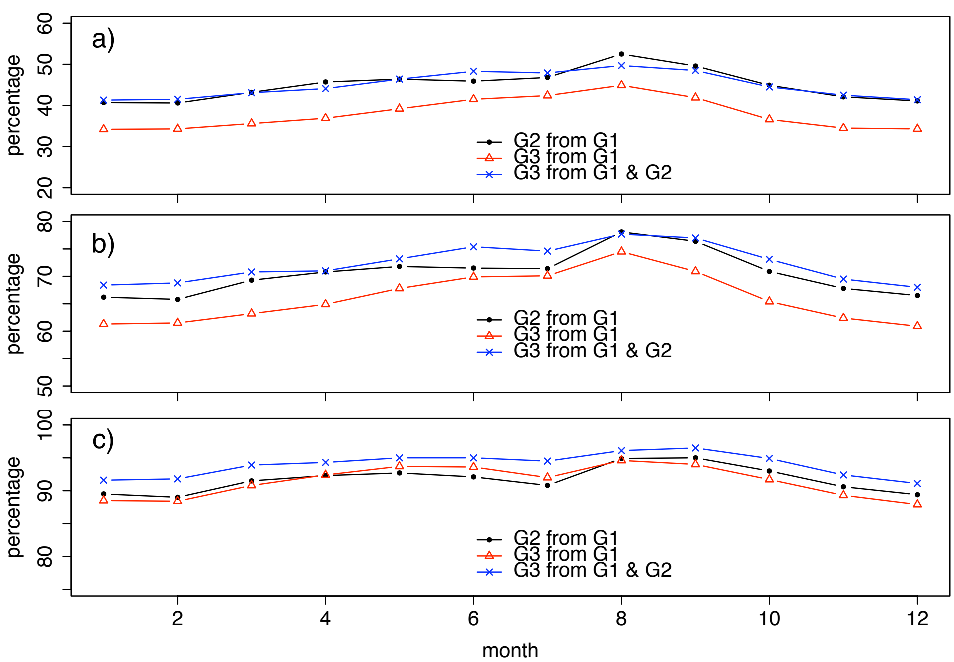

Figure 3. Percentage error estimates between ±0.5 °C (a), ±1 °C (b), ±2 °C (c) using a constant lapse rate at group-2 stations using group-1 stations (circles), group-3 stations using group-1 stations (triangles), group-3 stations using group-1 and group-2 stations (crosses). – *Hlutfallsleg skekkja í reiknuðum hita fyrir fast hitafall með hæð.*

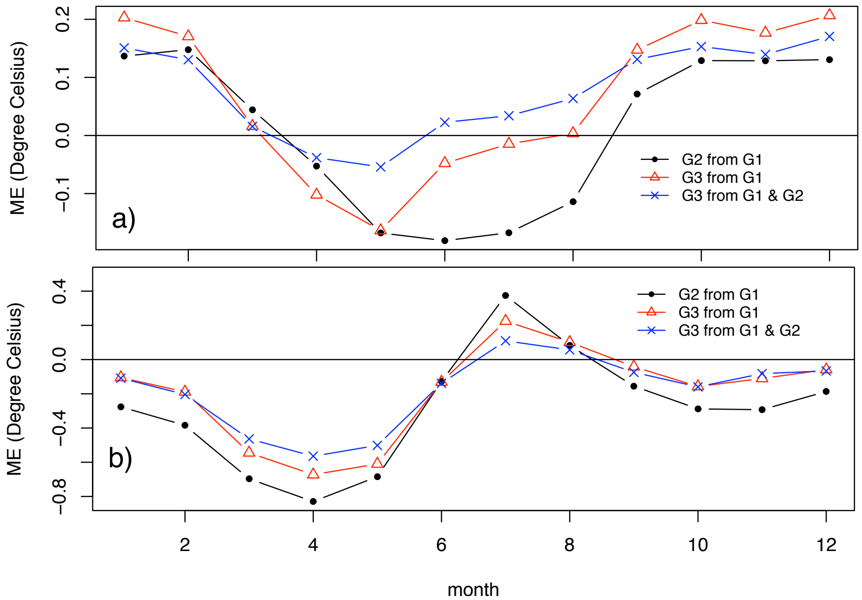

Figure 4. Mean error (ME) at stations below 300 m a.s.l. (a) and stations above 300 m a.s.l. (b) using a constant lapse rate at group-2 stations using group-1 stations (circles), group-3 stations using group-1 stations (triangles), group-3 stations using group-1 and group-2 stations (crosses). – *Meðalskekkja (ME) fyrir stöðvar neðan (a) og ofan (b) 300 m y.s. fyrir fast hitafall með hæð.*

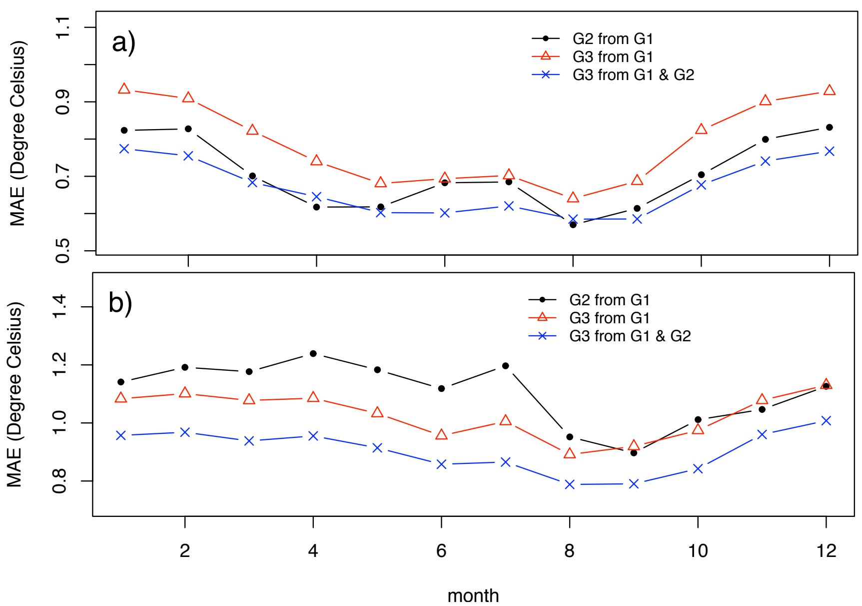

Figure 5. Mean absolute error (MAE) at stations below 300 m a.s.l. (a) and stations above 300 m a.s.l. (b) using a constant lapse rate at group-2 stations using group-1 stations (circles), group-3 stations using group-1 stations (triangles), group-3 stations using group-1 and group-2 stations (crosses). – *Meðaltal tölugildis skekkju (MAE) fyrir stöðvar neðan (a) og ofan (b) 300 m y.s. fyrir fast hitafall með hæð.*

from $-0.2\,^{\circ}\mathrm{C}$ to $0.2\,^{\circ}\mathrm{C}$. Above 300 m a.s.l., ME is mostly negative except in July and August and ranges from $-0.8\,^{\circ}\mathrm{C}$ to $0.4\,^{\circ}\mathrm{C}$. The mean error estimated at group-3 stations below and above 300 m a.s.l. is often less biased when the estimate is made with fields derived from group-1 and group-2 stations together than with group-1 stations only.

A similar seasonality is found for MAE below and above 300 m a.s.l., with better estimates in summer than in winter and an optimum around August and September. However, above 300 m a.s.l., spring MAE is as high as winter MAE, most likely because of the large negative spring ME, while it is lower below 300 m a.s.l. Errors are larger above 300 m a.s.l. than below 300 m a.s.l., most likely due to the reduction of station density with altitude. For stations below 300 m a.s.l., MAE is lower at group-2 stations than at group-3 stations when the temperature fields are estimated with group-1 stations, but above 300 m a.s.l., this is the other way around except from September to December where MAE is similar. Group-2 has some stations located above 300 m a.s.l. in the highlands, where few group-1 (manned) stations are available (Figure 1) while group-3 stations are usually located closer to the coast where the density of manned stations is large, leading to smaller horizontal interpolation errors. Spatial lapse rate variations between coastal and inland areas can also account for some of these errors, especially when coastal stations are used to interpolate farther inland.

Verification against independent stations using a temporally variable lapse rate

The benefit of using a temporally variable lapse rate (Table 3) was investigated. The resulting error statistics (Table 4) indicate that overall, the use of the variable lapse rate of Tveito *et al.* (2000) did not lead to an improvement except from March to May while it was observed to provide estimates of similar quality in summer and of worse quality in winter. First, ME derived from estimates made using only group-1 stations was found to be systematically positive and more often more biased at group-2 stations than ME derived from estimates made with the constant lapse rate, except in spring. At group-3 stations (not shown), ME was also observed to be systematically positive while ME corresponding to estimates made with a constant lapse rate was positive from July to February, negative otherwise and usually less biased except in spring. Similar results were observed for estimates made with group-1 and group-2 stations, and verified at group-3 stations (not shown). In all three cases, the largest differences between the two sets of ME were observed in spring and winter when the difference between constant and variable lapse rates are the largest. Results also indicate that estimates derived using a variable lapse rate have larger MAE and RMSE from November to February, slightly lower MAE and RMSE from March to May and similar MAE and RMSE from June to October than estimates made with the constant lapse rate (not shown).

Table 4. Error statistics at G-2 stations from G-1 stations using a variable lapse rate. – *Tölfræðileg dreifing skekkju á stöðvum í flokki 2 fyrir hita sem reiknaður er út frá stöðvum í flokki 1 fyrir breytilegt hitafall með hæð.*

Statistics/Period	Jan	Feb	Mar	Apr	May	Jun	Jul	Aug	Sep	Oct	Nov	Dec
ME	0.48	0.44	0.17	0.18	0.08	0.04	0.08	0.02	0.15	0.22	0.43	0.46
MAE	1.07	1.03	0.82	0.78	0.76	0.82	0.85	0.69	0.70	0.80	0.99	1.06
Percentage error within $\pm 0.5\,^{\circ}\mathrm{C}$	36.8	38.6	45.2	48.3	49.6	47	47	52.9	50.5	45.6	39.1	37.6
Percentage error within $\pm 1\,^{\circ}\mathrm{C}$	60.2	62.5	71.5	73.7	75.3	72.1	71.5	78.2	76.9	71.8	63.6	61
Percentage error within $\pm 2\,^{\circ}\mathrm{C}$	85	86	91.8	92.6	92.8	91.2	90.2	94.6	94.8	92.5	87.4	85.3

As mentioned earlier, monthly lapse rates derived from the analysis of Tveito *et al.* (2000) for Iceland were calculated as one of the components of a multiple linear regression (MLR) analysis between temperature and various topographic and geographic factors and these lapse rate estimates could be influenced by the presence of other variables in the MLR relationships which may make them non-optimal for this application. Moreover, long-term averaged conditions may not reflect spatio-temporal variations observed at daily time steps such as the presence of temperature inversions, lapse rate variations in space, for instance between windward/lee-side (Foehn effect) or when the meteorological situations are changing rapidly or are not homogeneous accross the country. Also, the seasonal lapse rates were derived from the synoptic and climatic network mainly located near the coastal and in lowland areas while the validation was made with the automatic network partly deployed inland and in more mountainous regions where local conditions may be different.

Finally, as mentioned before, the benefit of increasing the station density by combining group-1 and group-2 stations is evident and a large MAE reduction is observed at group-3 stations (not shown).

Comparison with reference climatology

Maps of 30-year mean monthly and annual temperature for the 1961–1990 period were calculated from the daily fields derived from group-1 stations with both constant and variable lapse rates and compared with the temperature fields of Björnsson *et al.* (2007). A visual inspection indicates a good overall resemblance between both sets of fields, although discrepancies can be found with a detailed comparison. Tables 5 and 6 present the statistics of the difference between the reference climatology and the two data sets for each month and Figure 6 presents maps of the difference between the reference climatology and (the constant lapse rate) estimates based on the daily fields for January, April, July and October. The results have a tendency similar as was found previously, namely that overall, estimates made with a variable lapse rate are not better than those made with a constant lapse rate of 6.5 °C/km.

Maps of the differences (Figure 6) indicate a tendency towards a slight underestimation (positive difference) near the coast and an overestimation (negative difference) in the innermost part of the country where the station density is lowest and for which both sets of maps are most uncertain. A large region where the difference is mainly negative develops from November to May and reaches its maximum spatial extent and magnitude in April, in the highlands, over Tröllaskagi and over the main ice caps. In July and August, the difference is mainly positive all over the country. The difference averaged over Iceland ranges from $-0.9\,^{\circ}$C to $0.3\,^{\circ}$C, with positive values in July and August and negative ones during the rest of the year, leading to slightly negative annual mean difference. The mean absolute difference is highest in spring, and ranges from $0.3\,^{\circ}$C in September to nearly $1.0\,^{\circ}$C in April. The proportion of differences within several temperature ranges was calculated over all grid points. The proportion of grid points within $\pm 0.5\,^{\circ}$C ranges from 35% in April to 82% in September, the proportion of grid points within $\pm 1\,^{\circ}$C ranges from 60% in April to 95% in September, and the proportion of grid points within $\pm 2\,^{\circ}$C ranges from 89% in April to 99% in September. For comparison, Björnsson *et al.* (2007) found that 90% of their 30-year mean monthly temperature estimates were accurate within $\pm 1\,^{\circ}$C in January and July. The difference between Björnsson's *et al.* maps and the temperature estimates presented in this study for these months are close to this error range (Table 5).

Thus, the gridded temperatures are unbiased in average within approximately $\pm 1\,^{\circ}$C. This is an important property of the data set for various hydrological and glaciological applications where systematic biases in input temperatures may lead to compensating errors in calibrated model parameters and consequently to errors in some model predictions, particularly climate change predictions.

ANOMALY MAPS

Daily temperature fields calculated with group-1 stations only and the constant lapse rate were used to derive 10-year mean annual temperature anomaly maps with respect to the 1961–1990 reference period for the

Table 5. 1961–1990 climatology: Statistics of differences between average temperature for the period 1961–1990 calculated by Björnsson *et al.* (2007) and calculated from the daily fields derived with a constant lapse rate. – *Veðurfar 1961–1990: Töluleg dreifing á mismun á meðalhita tímabilsins 1961-1990. Annars vegar er um að ræða hita sem reiknaður var af Halldóri Björnssyni o.fl. (2007) og hins vegar meðaltal daglega hitans sem hér er lýst fyrir fast hitafall með hæð.*

Statistics/Period	Jan	Feb	Mar	Apr	May	Jun	Jul	Aug	Sep	Oct	Nov	Dec
Mean difference	–0.35	–0.59	–0.79	–0.86	–0.56	–0.03	0.28	0.25	–0.07	–0.11	–0.26	–0.35
Mean absolute difference	0.52	0.71	0.87	0.95	0.71	0.39	0.52	0.45	0.30	0.35	0.45	0.52
Root Mean Square difference	0.7	0.9	1.12	1.23	0.97	0.58	0.69	0.61	0.45	0.50	0.60	0.67
Perc. difference within $\pm 0.5\,^{\circ}\mathrm{C}$	59.2	42.7	38.0	35.3	48.3	74.4	59.3	65.2	82.0	76.9	64.9	58.6
Perc. difference within $\pm 1\,^{\circ}\mathrm{C}$	86.8	72.7	64.1	60.3	72.6	92.0	87.9	90.3	95.3	94.1	91.3	87.2
Perc. difference within $\pm 2\,^{\circ}\mathrm{C}$	98.5	97.6	91.9	89.5	95.0	98.8	98.6	99.2	99.6	99.5	99.2	99.0

Table 6. 1961–1990 climatology: Statistics of differences between average temperature for the period 1961–1990 calculated by Björnsson *et al.* (2007) and calculated from the daily fields derived with variable lapse rates. – *Veðurfar 1961–1990: Töluleg dreifing á mismun á meðalhita tímabilsins 1961-1990. Annars vegar er um að ræða hita sem reiknaður var af Halldóri Björnssyni o.fl. (2007) og hins vegar meðaltal daglega hitans sem hér er lýst fyrir breytilegt hitafall með hæð.*

Statistics/Period	Jan	Feb	Mar	Apr	May	Jun	Jul	Aug	Sep	Oct	Nov	Dec
Mean difference	0.81	0.53	0.08	0.30	0.45	0.46	0.49	0.43	0.29	0.43	0.79	0.69
Mean absolute difference	0.99	0.75	0.49	0.64	0.70	0.65	0.68	0.59	0.44	0.58	0.94	0.86
Root mean square difference	1.40	1.07	0.69	0.92	0.97	0.87	0.88	0.78	0.62	0.81	1.34	1.22
Percentage difference within $\pm 0.5\,^{\circ}\mathrm{C}$	42.5	51.3	65.4	55.6	50.0	49.9	45.2	52.6	67.2	57.2	44.1	46.7
Percentage difference within $\pm 1\,^{\circ}\mathrm{C}$	63.6	73.4	87.4	78.9	75.7	79.5	78.1	82.6	89.5	81.6	65.3	68.3
Percentage difference within $\pm 2\,^{\circ}\mathrm{C}$	85.4	91.5	98.0	94.8	94.2	96.3	96.6	97.9	99.0	96.9	86.5	88.4

period 1951–2010 (Figure 7). First, monthly fields were derived by averaging daily temperature fields, then annual fields were derived by averaging these monthly fields and further averaged over the required period. The 1950s had a positive anomaly ranging mostly between $0.25\,^{\circ}\mathrm{C}$ and $1\,^{\circ}\mathrm{C}$, then the anomaly fluctuated between $\pm 0.5\,^{\circ}\mathrm{C}$, either homogeneously or with a dipole structure oriented N–S or NE–SW, until 1990 and becomes essentialy positive after that. The last decade in particular has seen the largest warming over the last 60 years, above $1\,^{\circ}\mathrm{C}$ with respect to 1961–1990 over a large part of the country. Long-term climate warming in Iceland due to increasing concentration of CO_2 in the atmosphere is likely to be 0.2 to $0.4\,^{\circ}\mathrm{C}$ per decade until 2050 (Nawri and Björnsson, 2010) but as can be seen from this analysis, natural climate variability even on a decadal time-scale can be larger than the effect of this estimated long-term trend over several decades.

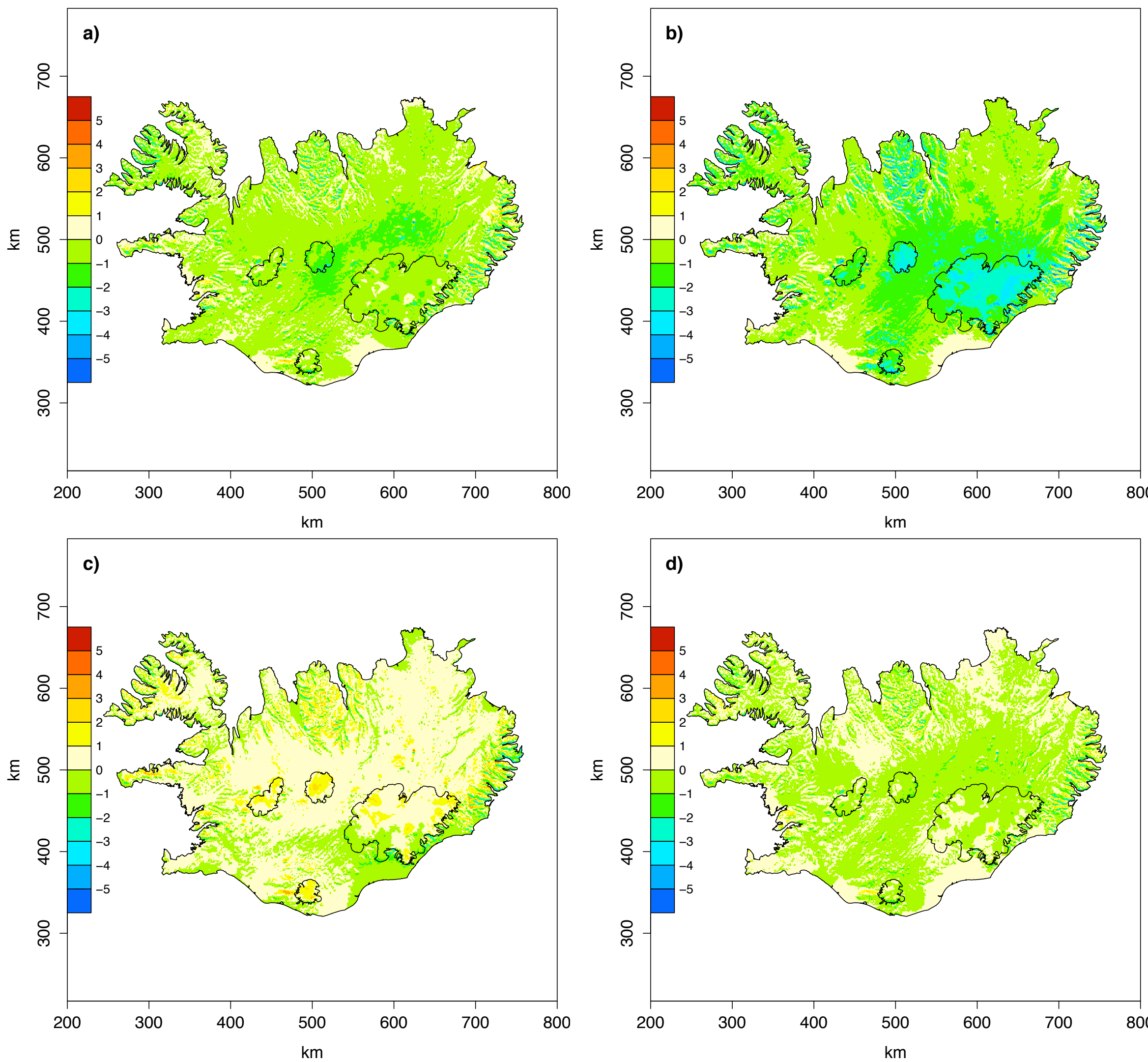

Figure 6. Difference (Degrees Celsius) in 1961–1990 mean monthly temperature for January (a), April (b), July (c) and October (d) between the analysis of Björnsson *et al.* (2007) and the analysis of this paper (see also table captions 5 and 6). The four main glaciers are also represented. – *Mismunur á meðalhita (°C) janúar (a), apríl (b), júlí (c) og október (d) fyrir tímabilið 1961–1990. Annars vegar er um að ræða hita sem reiknaður var af Halldóri Björnssyni o.fl. (2007) og hins vegar meðaltal daglega hitans sem hér er lýst.*

SUMMARY

A daily gridded temperature climatology with a 1 km resolution has been constructed for Iceland for the last 60 years. It is the first of its kind and publicly available in digital form. Although the procedure used to derive the data set is simple, validation of the temperature fields with independent observations shows that they are of reasonable quality and suitable for a broad range of applications, including glacier mass-balance

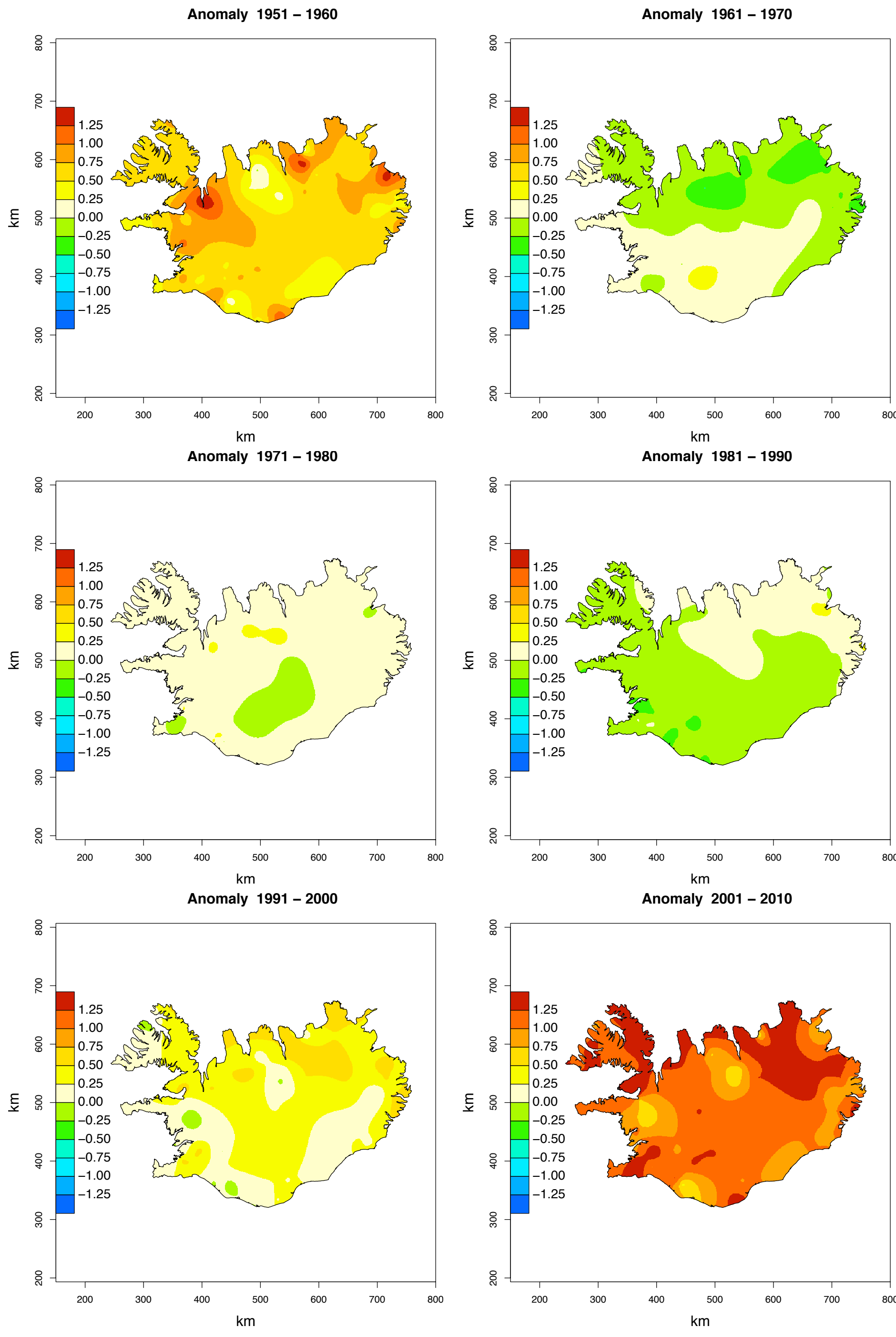

Figure 7. Decadal anomaly maps (Degrees Celsius) with respect to the standard reference period 1961–1990. Positive anomaly means warmer than reference period. – *Meðalhitavik (°C) áratuga frá meðaltali staðaltímabilsins 1961-1990. Jákvætt frávik þýðir að viðkomandi tímabil er hlýrra en staðaltímabilið.*

studies and climate change research. The data set reflects air-mass temperature conditions around and in the free-atmosphere over glaciers better than in-situ measurements of 2-m temperature on the glaciers themselves which are known to be damped by energy exchange processes near the melting ice surface (Guðmundsson *et al.*, 2009).

The quality of the temperature fields varies with season and location. Estimates near the coast and at low elevations are more accurate than in the highlands and at high elevations because of a more dense network. When using a constant lapse rate of $6.5\,^{\circ}$C/km, summer temperatures were found to be more accurate than winter temperatures and spring temperatures had the largest bias. The expanding network of automatic weather stations up to about 950 m a.s.l. in recent years was found to improve the estimated temperature fields. An attempt to use a seasonally variable lapse rate did only improve the quality of the temperature estimates during spring time and gave similar results in summer time. The 30-year mean monthly and annual maps derived from the daily temperature fields are in reasonable agreement with the earlier estimates of Björnsson *et al.* (2007) that were directly constructed from mean monthly station values employing a sophisticated interpolation method, reinforcing the credibility of the new data set.

The new temperature data set has already been used to study the impact of past temperature variations on hydrological systems in Iceland (Crochet, 2010) and it is currently used in hydrological modeling studies at IMO (Atladóttir *et al.*, 2011). It will be useful for climate analysis such as the validation of climate models and for the development of statistical downscaling methods of GCM or RCM projections (Engen-Skaugen, 2007). The spatial interpolation of daily temperature over the complex terrain of Iceland remains a challenge and further improvements to the methodology presented here will be investigated. One possible improvement is to estimate the surface lapse rate on a daily basis, from linear regression between observations and elevation or by optimization. Another possibility is to combine the temperature maps of Björnsson *et al.* (2007) with anomaly interpolation.

Acknowledgements

This study was carried out within the framework of the Nordic Climate and Energy System research project (CES) and the corresponding Icelandic national project (LOKS), whose main objectives are to make a comprehensive assessment of the impact of climate change on renewable energy resources in the Nordic countries. The CES project is funded by Nordic Energy Research and the Nordic energy sector while the LOKS project is funded by Landsvirkjun (the National Power Company of Iceland), the Icelandic Road Administration and the National Energy Authority.

The authors are grateful to Trausti Jónsson for numerous discussions and suggestions regarding this study and to Landsvirkjun, the Icelandic Road Administration, The National Energy Authority, The Icelandic Maritime Administration and local harbors for providing data. The authors would also like to thank the two anonymous reviewers for their helpful comments.

ÁGRIP

Daglegur yfirborðshiti á Íslandi hefur verið reiknaður á reglulegu reiknineti með mikilli upplausn fyrir tímabilið 1949–2010. Í 60–80% tilvika er reiknaði hitinn innan við $\pm 1\,^{\circ}$C og í 90–95% tilvika innan við $\pm 2\,^{\circ}$C frá óháðum hitamælingum á tímabilinu 1995–2010 (hlutfallið er breytilegt eftir mánuðum innan ársins). Reiknuðu hitagögnin henta því vel til ýmis konar líkanreikninga í vatnafræði, jöklafræði og veðurfarsfræði. Reiknaði hitinn fellur best að mældum hita nærri ströndum landsins vegna þess að þar eru hitamælingar þéttastar. Hitamælingar frá sjálfvirkum veðurstöðum, sem hafist var handa við að setja upp snemma á tíunda áratug síðustu aldar, bæta nákvæmni reiknaða hitans. Þrjátíu ára meðaltölum reiknaða hitans ber vel saman við kort af þrjátíu ára meðalhita sem reiknuð hafa verið út frá meðalhita mánaða á veðurstöðvum með vönduðum tölfræðilegum aðferðum. Greining á hitabreytingum milli áratuga á grundvelli reiknuðu hitagagnanna sýnir að áratugurinn 2001–2010 var hlýjasti áratugur síðustu 60 ára og gerir kleift að ákvarða breytileika í hlýnuninni milli svæða. Sem dæmi má nefna að hlýnun síðustu áratuga var meiri inn til landsins en við ströndina.

REFERENCES

Aðalgeirsdóttir, G., T. Jóhannesson, H. Björnsson and F. Pálsson 2006. Response of Hofsjökull and southern Vatnajökull, Iceland, to climate change. *J. Geophys. Res.* 111, F03001, doi:10.1029/2005JF000388.

Apaydin, H., F. K. Sonmez and Y. E. Yildirim 2004. Spatial interpolation techniques for climate data in GAP region in Turkey. *Clim. Res.* 28, 31–40.

Atladóttir, A., P. Crochet, S. Jónsson and H. B. Hróðmarsson 2011. *Mat á flóðagreiningu með rennslisröðum reiknuðum með vatnafræðilíkaninu WASIM. Frumniðurstöður fyrir vatnasvið á sunnanverðum Vestfjörðum.* Evaluation of flood estimation with discharge series generated with the WASIM hydrological model. A case study in the West Fjords, Iceland. Icel. Meteorol. Office, Rep. 2011-008 (in Icelandic), 41 pp.

Bergström, S., T. Jóhannesson, G. Aðalgeirsdóttir, A. Ahlström, L. M. Andreassen, J. Andréasson, S. Beldring, H. Björnsson, B. Carlsson, P. Crochet, M. de Woul, B. Einarsson, H. Elvehøy, G. E. Flowers, P. Graham, G. O. Gröndal, S. Guðmundsson, S.-S. Hellström, R. Hock, P. Holmlund, J. F. Jónsdóttir, F. Pálsson, V. Radic, L. A. Roald, J. Rosberg, S. Rogozova, O. Sigurðsson, M. Suomalainen, Th. Thorsteinsson, B. Vehviläinen and N. Vehviläinen 2007. *Impacts of climate change on river runoff, glaciers and hydropower in the Nordic area. Joint final report from the CE Hydrological Models and Snow and Ice Groups.* Reykjavík, Climate and Energy, Rep. CE-6, 40 pp.

Björnsson, H., T. Jónsson, S. S. Gylfadóttir and E. O. Ólason 2007. Mapping the annual cycle of temperature in Iceland. *Meteorol. Zeitschrift* 16, 45–56.

Bolstad P. V., L. Swift, F. Collins and J. Régnière 1998. Measured and predicted air temperatures at basin to regional scales in the southern Appalachian mountains. *Agric. For. Meteorol.* 91, 161–176.

Chuanyan, Z., N. Zhongren and C. Guodong 2005. Methods for modelling of temporal and spatial distribution of air temperature at landscape scale in the southern Qilian mountains, China. *Ecol. Model.* 189, 209–220.

Creutin, J. D. and C. Obled 1982. Objective analyses and mapping techniques for rainfall fields: An objective comparison. *Water Resour. Res.* 18 (2), 413–431.

Crochet, P. 2010. Impact of historic climate variations on streamflow characteristics in Icelandic rivers. *Proceedings from the conference: Future climate and renewable energy: impacts, risks and adaptation*, Oslo, Norway, 31 May – 2 June 2010, 12–13.

Crochet, P., T. Jóhannesson, T. Jónsson, O. Sigurðsson, H. Björnsson, F. Pálsson and I. Barstad 2007. Estimating the spatial distribution of precipitation in Iceland using a linear model of orographic precipitation. *J. Hydrometeorol.* 8, 1285–1306.

Daly, C. 2006. Guidelines for assessing the suitability of spatial climate data sets. *Int. J. Climatol.* 26, 707–721.

Dodson, R. and D. Marks 1997. Daily air temperature interpolated at high spatial resolution over a large mountainous region. *Climate Research* 8, 1–20.

Einarsson, B. and S. Jónsson 2010. *The effect of climate change on runoff from two watersheds in Iceland.* Reykjavík, Icel. Meteorol. Office, Rep. 2010-016, 34 pp.

Engen-Skaugen, T. 2007. Refinement of dynamically downscaled precipitation and temperature scenarios. *Clim. Change* 84, 365–382.

Gozzini, B., A. Crisci, D. Bertini, F. Maselli, F. Meneguzzo, G. Zipoli, S. Paniagua, V. Perarnaud, K. Van Diepen, H. Boogard, D. Courault and R. Delecolle 2000. *Coordination and comparison of several interpolation methods of meteorological data (minimum temperature).* COST Action 79. EUR 19545, 102 pp.

Guðmundsson, S., H. Björnsson, F. Pálsson and H. H. Haraldsson 2009. Comparison of energy balance and degree-day models of summer ablation on the Langjökull ice cap, SW Iceland. *Jökull* 59, 1–18.

Hasenauer, H., K. Merganicova, R. Petritsch, S. A. Pietsch and P. E. Thornton 2003. Validating daily climate interpolations over complex terrain in Austria. *Agric. For. Meteorol.* 119, 87–107.

Hebeler, F. and R. S. Purves 2008. The influence of resolution and topographic uncertainty on melt modelling using hypsometric sub-grid parameterization. *Hydrol. Proc.* 22, 3965–3979.

Hovmöller, E. 1960. *Climatological information on Iceland.* United Nations report no. TAO/ICE/4, 115 pp.

Hudson, G. and H. Wackernagel 1994. Mapping temperature using kriging with external drift: theory and an example from Scotland. *Int. J. Climatol.* 14, 77–91.

Jóhannesson, T. 1997. The response of two Icelandic glaciers to climatic warming computed with a degree-day mass-balance model coupled to a dynamic glacier model. *J. Glaciol.* 43, 321–327.

Jóhannesson, T., O. Sigurðsson, T. Laumann and M. Kennett 1995. Degree-day mass balance modelling with applications to glaciers in Iceland, Norway and Greenland. *J. Glaciol.* 41, 345–358.

Jóhannesson, T., G. Aðalgeirsdóttir, H. Björnsson, P. Crochet, E. B. Elíasson, S. Guðmundsson, J. F. Jónsdóttir, H. Ólafsson, F. Pálsson, Ó. Rögnvaldsson, O. Sigurðsson, Á. Snorrason, Ó. G. Blöndal Sveinsson and Th. Thorsteinsson 2007. *Effect of climate change on hydrology and hydro-resources in Iceland.* Reykjavík, Nat. Energy Authority, Rep. OS-2007/011, 91 pp.

Jónsdóttir, J. F. 2008. A runoff map based on numerically simulated precipitation and a projection of future runoff in Iceland. *Hydrol. Sci. J.* 53, 100–111.

Jónsdóttir, J. F., C. B. Uvo and R. T. Clarke 2008. Trend analysis in Icelandic discharge, temperature and precipitation series by parametric methods. *Hydrology Research* 39, 425–436.

Lebel, T., G. Bastin, C. Obled and J. D. Creutin 1987. On the accuracy of areal rainfall estimation: A case study. *Water Res. Res.* 23, 2123–2134.

Li, X. and M. W. Williams 2008. Snowmelt runoff modelling in an arid mountain watershed, Tarim basin, China. *Hydrol. Proc.* 22, 3931–3940.

Michlmayr, G., M. Lehning, G. Koboltschnig, H. Holzmann, M. Zappa, R. Mott and W. Schöner 2008. Application of the Alpine 3D model for glacier mass balance and glacier runoff studies at Goldbergkees, Austria. *Hydrol. Proc.* 22, 3941–3949.

Nawri, N. and H. Björnsson 2010. *Surface air temperature and precipitation trends for Iceland in the 21st century.* Reykjavík, Icelandic Meteorological Office, Rep. 2010-005, 42 pp.

Obleitner, F. 2000. The energy budget of snow and ice at Breiðamerkurjökull, Vatnajökull, Iceland. *Boundary-Layer Meteorology* 97, 385–410.

Pardo-Iguzquiza, E. 1998. Comparison of geostatistical methods for estimating the areal average climatological rainfall mean using data on precipitation and topography. *Int. J. Climatol.* 18, 1031–1047.

Phillips, D. L., J. Dolph and D. Marks 1992. A comparison of geostatistical procedures for spatial analysis of precipitation in mountainous terrain. *Agric. For. Meteorol.* 58, 119–141.

Price, D. T., D. W. McKenney, I. A. Nalder, M. F. Hutchinson and J. L. Kesteven 2000. A comparison of two statistical methods for spatial interpolation of Canadian monthly mean climate data. *Agric. For. Meteorol.* 101, 81–94.

Sharples, J. J., M. F. Hutchinson and D. R. Jellett 2005. On the horizontal scale of elevation dependence of Australian monthly precipitation. *J. Appl. Meteor.* 44, 1850–1865.

Smith, W. H. F. and P. Wessel 1990. Gridding with continuous curvature splines in tension. *Geophysics* 55, 293–305.

Stone, P. H. and J. H. Carlson 1979. Atmospheric lapse rate regimes and their parameterization. *J. Atmos. Sci.* 36, 415–423.

Tveito, O. E., E. Førland, R. Heino, I. Hanssen-Bauer, H. Alexandersson, B. Dahlström, A. Drebs, C. Kern-Hansen, T. Jónsson, E. Vaarby Laursen and Y. Westman 2000. *Nordic temperature maps. DNMI report 09/00.*, 52 pp.